Nucleolipid membranes: structure and molecular recognition

2008 J. Phys.: Condens. Matter 20 104212

(http://iopscience.iop.org/0953-8984/20/10/104212)

IOP Publishing Journal of Physics: Condensed Matter

J. Phys.: Condens. Matter **20** (2008) 104212 (8pp) doi:10.1088/0953-8984/20/10/104212

Nucleolipid membranes: structure and molecular recognition

S Milani[1], F Baldelli Bombelli[1], D Berti[1], S Dante[2], T Hauß[2,3] and P Baglioni[1]

[1] Department of Chemistry and CSGI (Consorzio Interuniversitario per lo sviluppo dei Sistemi a Grande Interfase), University of Florence, via Della Lastruccia 3, Sesto Fiorentino, Florence, Italy

[2] Hahn-Meitner-Institut, Berlin, Germany

[3] TU-Darmstadt, Darmstadt, Germany

E-mail: berti@csgi.unifi.it

Received 16 July 2007, in final form 18 September 2007
Published 19 February 2008
Online at stacks.iop.org/JPhysCM/20/104212

Abstract

Nucleolipid bilayers have been investigated through neutron diffraction, DSC and FTIR techniques. Two nucleolipids, bearing complementary RNA bases, have been chosen to highlight in their mixtures non-ideal behaviors ascribable to attractive interactions of the same selectivity and stoichiometry as in nucleic acids.

1. Introduction

Amphiphilic self-assemblies display a rich phase behavior, characterized by a large structural diversity, in terms of size, shape and interfacial flexibility of the aggregates. The typical independent parameters of the amphiphilic phase diagram are surfactant volume fraction, temperature and ionic strength: subtle variations of local microstructure can lead to cascade effects with dramatic morphological transitions on the mesoscale [1]. This feature lends itself to a bottom-up route to nanostructured assemblies, and can be further integrated by insertion of suitable functional motifs into the amphiphilic building block. This approach has led to the relatively new field of functional surfactants [2, 3], where an additional control parameter (i.e. photosensitivity [4], redox activity [5], molecular recognition, etc) is chemically encoded in the amphiphile. The ability to exploit the self-organization of functional assembling molecular building blocks and the possibility to impart tuneable, responsive properties to the resulting aggregates has led to a dramatic growth in the activity and understanding of this area. Among the biologically inspired examples, peptide amphiphiles [6] and oligonucleotide amphiphiles [7, 8] represent the most interesting and recent cases. The possibility to integrate nucleic motifs into amphiphilic molecules and use the know-how of soft matter to engineer nano-objects with nucleic decoration can ultimately lead to extremely complex and fascinating structures.

We are particularly interested in phosphatidyl nucleosides, where a nucleic acid monomer (i.e. a nucleotide) is conjugated to a double-chain lipid skeleton. These derivatives self-organize in aqueous solution as assemblies of various size, shape and interfacial curvature, according to the length of the two hydrophobic portions [9].

A coarse-grained mapping of their phase behavior can be performed by comparison with the synthetic precursor phosphatidylcholines: as the hydrophobic double chain is increased (i.e. the surfactant packing parameter $p = a_0 l_c / v$ decreases) we will observe the usual phase progression, from positively curved surfactant films (globular micelles) to flat assemblies (bilayers). However, with respect to lecithins, we introduce a globally anionic and bulkier head group that can consistently alter phase behavior. Moreover, since the geometry of spontaneous self-assembly and interfacial film properties are the result of a delicate balance between hydrophobic forces and polar head interactions, the properties of such self-assemblies can be further modulated by base–base interactions, that are triggered by aggregation.

Another interesting property of these nucleolipid assemblies concerns their complexation with single-stranded nucleic acids. We have recently found that diC_8P-adenosine (1-2-dioctanoyl-phosphatidyl-adenosine) globular micelles interact with ss-polyuridylic acid (polyU) to form superstructures that eventually evolve into a hexagonal mesophase, where the biopolymer is confined between cylindrical micelles [10]. The driving force for complexation is provided by molecular recog-

nition, as can be deduced from experiments performed on non-complementary partners. Similarly, when POPA (1-palmitoyl-2-oleoyl-phosphatidyl-adenosine) bilayers are swollen and annealed with a physiological buffer containing polyU, an increase of smectic period and appearance of a reflection due to the biopolymer ordering is observed [11]. The formation of biopolymer/lipid hybrid superstructures is by no means obvious, considering the like charge that normally prevents surfactant–polymer interactions.

Such structural complexity requires an in-depth structural characterization, necessary to highlight the contribution of base–base interactions to the overall properties of the assemblies.

This contribution is focused on the structural properties of mixed POPN bilayers. For this purpose, we have selected two bases that are complementary in RNA, adenosine and uridine.

Such mixtures have been studied for two different molar ratios and the properties on the mesoscale are correlated with details at a molecular level obtained through infrared spectroscopy.

2. Experimental section

2.1. Materials

1-palmitoyl-2-oleoyl-*sn*-glycero-3-phosphocholine (POPC) was purchased from Avanti Polar Lipids (Alabaster, AL, USA) and its purity checked by TLC. The lecithin was used as received since no oxidation or lyso products could be detected. Adenosine, uridine, HCl, $CHCl_3$, MeOH, and NH_3 (30% aqueous solution) used in the synthesis were purchased from Panreac (Spain). Phospholipase D from *Streptomyces sp.* AA586 was a generous gift from Asahi Chemical Industry Co., Ltd (Tokyo, Japan). Deuterium oxide (>99.5%) for neutron diffraction measurements was provided by Euriso-Top (Saclay, Gif sur Yvette, France). Tris buffer was purchased from Sigma-Aldrich.

POPU and POPA were synthesized starting from the corresponding phosphatidylcholine in a two-phase system [12] according to a modification of the method proposed by Shuto and co-workers [13, 14] and obtained as an ammonium salt. Separation from the by-products was achieved by silica-gel flash chromatography. Then POPA ammonium salt was transformed into sodium salt by titration. Purity was checked by TLC, ^{1}H NMR and elementary analysis.

2.2. Sample preparation

About 10 mg of POPN (N = adenosine or uridine) sodium salt was weighed. The amount of solution (Tris buffer 0.1 M) required to obtain the correct lipid/water content was added by weighing and the sample homogenized by several cycles of centrifugation followed by freeze/thaw treatment to obtain a paste. Besides POPU and POPA binary phases, two POPN mixtures were also characterized (POPA:POPU = 1:1 and POPA:POPU = 2:1).

2.2.1. Neutron diffraction. Since the spontaneous water sorption is different for the two binary systems, an intermediate hydration degree was chosen as a starting point for the structural characterization of the mixture (n_w = 13, lipid/water = 80:20). The pastes (80:20 = lipid:water w/w) were sandwiched between quartz slides (Hellma 45 × 1 × 0.01 mm). Full hydration of the same samples was then obtained placing the samples in an aluminum container saturated at 100% humidity for at least 12 h.

2.2.2. FTIR. The pastes (80:20 = lipid:water w/w) were sandwiched between CaF_2 windows.

2.2.3. DSC. About 5 mg of lyophilized powders was weighed; the appropriate amount of solution was added directly to the pan and the sample equilibrated with several cycles of freeze and thaw performed in the DSC apparatus.

2.3. Methods

2.3.1. Neutron diffraction data acquisition and data analysis. Neutron diffraction measurements have been performed at the membrane diffractometer V1 at the Berlin Neutron Scattering Center of the Hahn–Meitner Institute. Contrast variation was achieved using three different D_2O:H_2O compositions (i.e. 80:20, 50:50, 8:92). The water bath at the base of the chamber, used during the equilibration procedure, was also changed to hold the right contrast.

The temperature was kept constant at 25 °C during the measurement. Diffraction patterns were measured with rocking scans, rocking the sample around the expected Bragg position θ by $\theta \pm 2°$. The duration of the scans ranged between 30 min and 2 h, depending on the intensities of the reflections. The lamellar spacing d of each sample was calculated by the Bragg equation $n\lambda = 2d \sin\theta$, where n is the diffraction order and λ is the selected neutron wavelength (5.23 Å).

The standard method for analyzing bilayer structures is to construct scattering length density profiles, $\rho(z)$ equation (1), on an arbitrary relative scale by means of the Fourier transformation of the structure factor $F(h)$.

$$\rho(z) = \frac{2}{d}\sum_{h=1}^{n} F(h)\cos\left(\frac{2\pi hz}{d}\right) \qquad (1)$$

where F is in units of scattering lengths.

Integrated intensities were calculated with Gaussian fits to the experimental Bragg reflections. Absorption and Lorentz corrections were applied and the intensities square rooted to produce structure factor amplitudes $F(h)$.

The phase assignment was determined by analyzing the D_2O:H_2O exchange by means of the isomorphous replacement method, since the structure factors are a linear function of the mole fraction of D_2O:H_2O [15].

For data treatment only the structure factors determined at 8% D_2O were used. At this D_2O:H_2O contrast in fact the scattering length density of water is equal to zero and the scattering length density profiles describe the lipid bilayer only.

2.3.2. FTIR data acquisition and data analysis. IR spectra were collected with a Nexus 870 spectrophotometer (Thermo Nicolet, Paris) Transmittance spectra were recorded with 4 cm^{-1} resolution and 256 scans using a pyroelectric detector (DTGS-TEC).

Some regions of IR transmittance spectra were deconvolved by Gaussians in order to assign vibrational bands and to highlight possible shifts. Mainly, the absorption between 1800–1550 cm^{-1} is due to several vibrations of both nucleic acid headgroup and lipid tail. The number of fitting functions was chosen in agreement with the conventional literature both for the lipid and nucleic acids.

Vibrational dichroism experiments were achieved by using an external module equipped with a liquid nitrogen cooled mercury cadmium telluride (MCT) detector and a photoelastic modulator (Hinds instrument PEM90). All dichroic spectra were recorded with 8 cm^{-1} resolution and averaging 2000 scans.

Linear dichroism (LD), i.e. the different absorption of light polarized parallel and perpendicular with respect to an orientation direction, is related to the oscillatory strength of a transition and to the polarization of the transition with respect to the orientation axis. The LD signal ($LD = A_p - A_s$ where A_p and A_s are the absorbance in the parallel and perpendicular direction, respectively) is non-zero when the sample has a non-random orientation, as in the case of membrane layers.

During the vibrational linear dichroism (VLD) experiments, the angle between the membrane normal and the incoming beam was set at 40°. Membranes have linear dichroism equal to zero when the incoming beam is coincident with the membrane normal; however, they yield linear dichroic signal when the sample orientation is varied [16].

2.3.3. DSC. Thermal experiments were performed with a DSC-Q1000 differential scanning calorimeter (TA Instruments) using heating and cooling rates of 5 and 0.5 °C min^{-1}. Every sample was studied in the temperature range from −15 to 50 °C. At least two runs were recorded for each sample. The sample purity, after thermal analysis, was checked by TLC in order to verify possible lipid degradation.

2.3.4. Small angle x-ray diffraction (SAXD). SAXD experiments were performed on a SAXS-WAXS Hecus x-ray system GMBH (Graz, Austria) containing 1024 channels. The working q-range was 0.05–6 nm^{-1}, corresponding to Bragg's spacing of 120–1 nm. Cu Kα radiation of wavelength 1.542 Å was provided by a Seifert x-ray generator operated at 40 kV 10 mA. The samples were mounted in a Kapton sample holder. To minimize scattering from air, the camera volume was kept under vacuum during the measurements. Temperature control within 0.1 °C was achieved using a Peltier element.

3. Results and discussion

The study here presented was prompted by a recent investigation [17], where neutron diffraction pointed out that POPU and POPA lamellae have different lyotropic behaviors: when exposed to 98% R.H. they display different degrees of water sorption ($n_w = 17$ for POPU; $n_w = 9$ for POPA). Given the close similarity of the two headgroups, this difference can only be explained by a different interfacial organization of the two amphiphiles, possibly due to a network of self-stacking and/or H-bonding operating on the bilayer surface. FTIR linear dichroism supported this interpretation, highlighting different orientations of the base planes with respect to the bilayer normal.

Table 1. Bilayer spacing versus water content as determined by SAXS.

Lipid/water % (w/w)	n_w	POPA d (Å)	POPU d (Å)
Dry	0 ± 2	41.7 ± 0.5	47.0 ± 0.5
0.10	7 ± 2	47.5 ± 0.5	47.5 ± 0.5
0.15	9 ± 2	48.0 ± 0.5	48.5 ± 0.5
0.20	13 ± 2	48.5 ± 0.5	49.0 ± 0.5
0.25	17 ± 2	#	49.7 ± 0.5
0.30	22 ± 2	48.7 ± 0.5	50.0 ± 0.5
0.40	34 ± 2	48.5 ± 0.5	58.5 ± 0.5
0.50	51 ± 2	49.0 ± 0.5	69.0 ± 0.5
0.60	79 ± 2	50.0 ± 0.5	#
0.70	123 ± 2	49.5 ± 0.5	#

We have already reported that mixed vesicles made of DOP-adenosine and DOP-uridine present spectroscopic properties typical of the A–U molecular recognition pattern. Moreover mixed monolayers of the same derivatives, organized at the air/water interface, show deviations from ideal behavior in terms of cross-sectional area per lipid molecule, especially for the sample DOPA:DOPU = 1:2 [18]. Therefore, our attention has been focused on mixed POPA:POPU lamellar phases at two different molar ratios, with the purpose to ascertain a possible structural modulation induced by molecular recognition in lamellar phases.

Before comparing the mixtures to the pure nucleolipids, the structural properties of the binary mesophases have been characterized both above and below the water sorption threshold. The bilayer spacing (d) progression as a function of the water content was measured from SAXS experiments (table 1). The expected behavior for POPA and POPU, i.e. anionic lipids, is an unlimited swelling: water goes in between the bilayers that come apart infinitely due to double-layer electrostatic repulsion and eventually peel off. Zwitterionic lipids, such as POPC, show a swelling limit above which water imbibed forms an excess fluid phase between the bilayers [19]. The bilayer thickness, d_L, determined for POPU from the observed smectic period, knowing the surfactant volume fraction ϕ_L, shows an asymptotic trend if reported versus the number of water molecules. When d_L approaches its limiting value, 'full hydration' of the lipid polar head is reached: the solvent distributes in the interbilayer space, without altering the local bilayer structure (figure 1). The number of water molecules per lipid necessary to attain 'full hydration' conditions is in perfect agreement with gravimetric measurements performed on bilayers made of the ammonium salt of POPU, pointing out no particular effect of the nature of the counter-ion on phase behavior.

POPA lamellae show on the contrary an unexpected lyotropic behavior. The progression of the structural

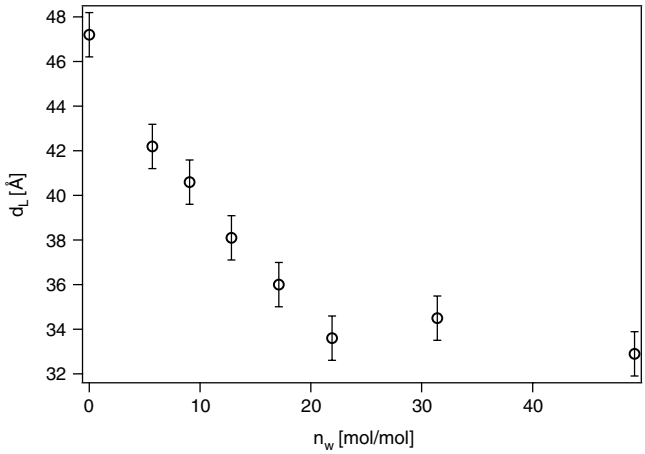

Figure 1. Bilayer thickness d_L versus the number of water molecules (n_w) for POPU lamellar phases.

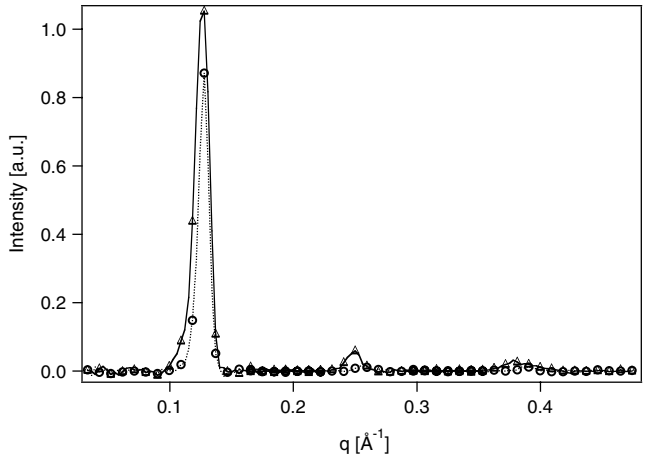

Figure 2. Diffraction patterns of mixture 8% D_2O at full hydration: (△) POPA:POPU 1:2, (○) POPA:POPU 1:1.

parameters resembles the trend observed for neutral lipids, with a swelling limit above which the excess water separates as a fluid phase. A reasonable working hypothesis for such a peculiar behavior might be again related to the stacking constant of the adenosine motif. It is well known from NMR experiments that stacking interactions among nucleic bases follow the trend purine–purine > purine–pyrimidine > pyrimidine–pyrimidine [14, 20]. This might cause favorable interbilayer interactions that could partially oppose double-layer repulsion and hinder interbilayer water insertion. Besides this noteworthy difference, neutron diffraction rocking scans reveal an almost powder-like nature of POPA membranes, in agreement with a different long-range order of the two nucleolipids, showing five diffraction patterns for POPU and only three for POPA (data not shown). The higher long-range order of POPU bilayers with respect to POPA is a general feature, and had already been noticed for the NH_4^+ salts, as illustrated in a previous report [17].

It is then interesting to investigate the behavior for the mixed systems. Figure 2 shows the neutron diffraction spectra from the two different nucleolipid mixtures,

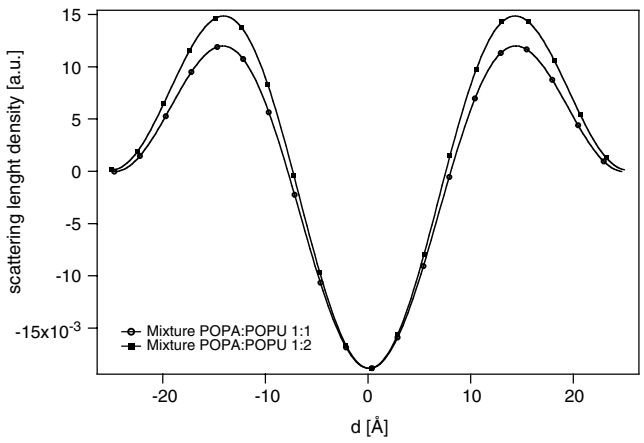

Figure 3. Experimental scattering length density profiles at 8% D_2O from diffraction data of POPA:POPU membrane mixtures.

POPA:POPU = 1:2 and POPA:POPU = 1:1, at full hydration. Similar results have been obtained for the analogous 80:20 samples. The single lamellar phase detected confirms the miscibility of the two lipids, as should be expected from the similar chemical natures.

The number of reflections observed is only three, as for the POPA binary system. Therefore, POPA provides the imprinting for long-range ordering. The spacing of the mesophases depends on the contrary on POPU molar ratio, being higher for higher POPU content. A coarse-grained scattering length density profile along the normal to the membrane plane can be obtained through Fourier synthesis from the structure factor at 8% D_2O /92% H_2O, notwithstanding the limited number of reflections (figure 3). A typical lipid membrane profile shows two maxima corresponding the glycerol backbones of the lipids (representing therefore the lipid headgroups) and a minimum at the bilayer center, corresponding to the terminal methyl groups. These profiles characterize the elementary cell (*d* spacing) of the oriented samples composed of one bilayer with its hydration shell. The water content is centered at two edges of the diagram.

Observing the width of the peaks in figure 2, we notice that the mixture with higher POPU ratio shows a better alignment of the sample, as confirmed by the rocking scans performed around the first Bragg reflection (data not shown).

The mixed lamellar phase shows, for both molar ratios, a lower smectic period than the two binary systems, independently of the water content (20% w/w or full hydration). This implies a lower thickness for the lipid bilayer in the two cases. Given that the apolar portions of the amphiphiles are the same, this finding implies a structural modification in the polar head region, that can be explained only invoking different intermolecular interactions for the mixed systems with respect to binary samples. These interactions among bases can possibly involve a different orientation of the bases with respect to the membrane normal. The low resolution of the bilayer profile does not allow us to speculate further on this point; however, we can consider the average lipid cross-sectional area (table 2); the

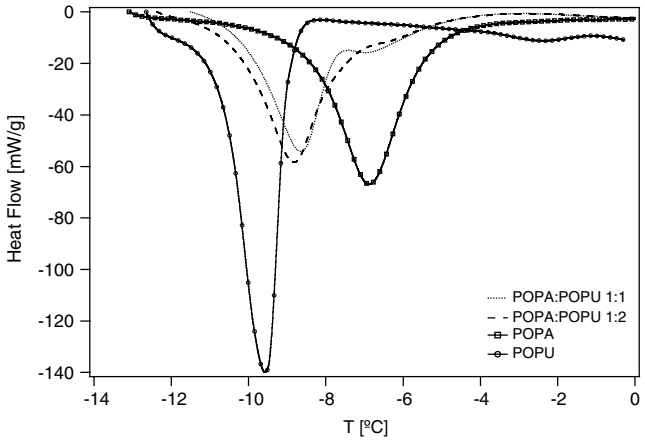

Figure 4. Differential scanning calorimetry heating curves for POPA:POPU membrane mixtures and POPA and POPU pure membranes at lipid/water 80/20 % (w/w).

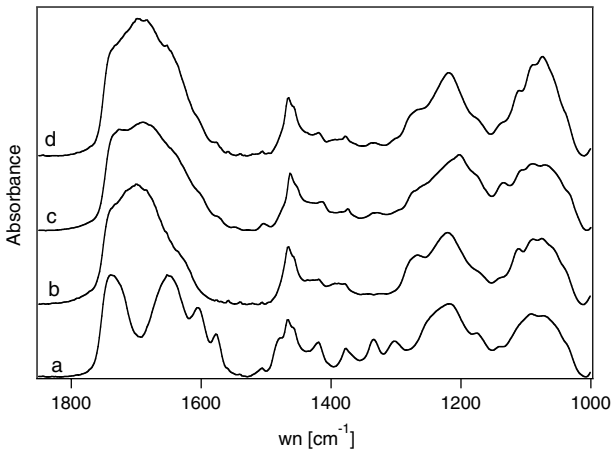

Figure 5. Infrared absorption spectra of (a) POPA, (b) POPU, (c) mixture POPA:POPU 1:1 and (d) mixture POPA:POPU 1:2 bilayers at lipid/water 80/20 % (w/w). The curves were shifted along the left axis to increase graphic readability.

Table 2. Bilayer thickness and area for polar headgroup at 80/20 lipid/water % (w/w).

Lipid	d_L (Å)	Area (Å^2)
POPA	38.1 ± 0.5	72 ± 2
POPU	38.5 ± 0.5	70 ± 2
POPU:POPA 1:1	37.3 ± 0.5	73 ± 2
POPU:POPA 2:1	37.3 ± 0.5	72 ± 2

area per lipid can be evaluated as the simplest measure of lateral organization. This calculation requires an accurate knowledge of molecular volumes, evaluated in our case for the two lipids as previously reported [17]. We are aware that its determination in a lipid mixture is not trivial, but the correspondence of the chemical structure of the two lipids, except the nucleic base, makes this parameter valuable.

As table 2 reveals, the mixed lamellar phases show no striking structural deviations from binary systems. Based on molar ratio weighted averages, the cross-sectional lipid area is higher for both mixtures than for POPA and POPU, indicating a different orientation of the bases.

DSC experiments were performed to further clarify this behavior [21–23]. Figure 4 shows the endothermic curves obtained for POPA and POPU binary membranes and their mixtures. The area between the experimental curve and an interpolated baseline corresponds to the heat of transition from the gel to liquid crystalline phases. The main transition temperatures, T_m, are $-6.8\,^\circ$C and $-9.6\,^\circ$C for POPA and POPU respectively. This difference, which roughly holds independently of the hydration degree, again reveals a different lateral organization for the two membranes, especially striking considering the identity of the chains and charge and the extremely similar steric hindrance [22, 24]. The presence of stronger intermolecular interactions for POPA than POPU is therefore maximized in the more ordered gel phase. The widths of DSC curves for the binary nucleolipid membranes highlight the higher cooperativity for the L_β–L_α transition for POPU lamellae. This observation agrees with the structural information obtained by neutron diffraction for this latter lipid, where a higher mosaicity was noticed. If we now consider the mixtures, we notice for both molar ratios one broad endothermic peak centered between the endothermic peaks of the pure lipids. The T_m for POPA:POPU 1:1 membranes is about $-8.5\,^\circ$C and that for POPA:POPU 1:2 is $-8.9\,^\circ$C, closer to the POPU one. Moreover, the calorimetric curves for both mixtures show a small shoulder above the main transition, more pronounced for the 1:1 ratio. These shoulders clearly recall the POPA binary lamellar phase, indicating that there are POPA rafts in the gel phase. However, given the limited temperature range accessible for the neutron scattering experiments, we could not verify the diffraction pattern for the mixed gels: the only evidence that we have is that the sample is monophasic in the liquid crystalline domain, but we cannot rule out any clustering of like molecules along the membrane plane.

The main transition temperatures of the mixed membranes do not scale linearly with lipid compositions and are therefore not ideal; however, given the width of the peaks, it is not obvious to apply current theories of lipid mixtures to infer the non-ideality parameter [25–30], which is normally determined for mixed lamellar phases, whose transition temperatures are widely spaced on the T axis.

To get further insight on base–base interactions, FTIR measurements were carried out. IR is a powerful technique to analyze intermolecular and intramolecular hydrogen bonds and has been especially and extensively used to study nucleic acids or nucleosides [31–35]. The region between 1700 and 1550 cm^{-1} is surely the most interesting for this issue [36, 37]. Therefore, we have recorded IR spectra on pure and mixed nucleolipid lamellar phases (figure 5) to detect possible band shifts in this region. However, a large number of vibration modes both of the lipid and of the nucleic acid occurs in this region [36, 38], making a straightforward interpretation of the experimental data difficult. Figure 5 shows that the spectra are characterized by an extremely broad band (except for POPA), where it is difficult even to make out the contributions of the single transitions.

Table 3. Infrared absorption spectra fitting results.

POPA calculated frequency (cm^{-1})	POPU calculated frequency (cm^{-1})	POPA:POPU 1:1 calculated frequency (cm^{-1})	POPA:POPU 2:1 calculated frequency (cm^{-1})	Vibration mode attribution
1778	1760	1760	1765	
1746	1745	1747	1745	ν C=O carboxylic tails
1730	1730	1735	1730	ν CO–O carbonylic tails
	1705	1706	1702	ν C_2=O uridine
		1690	1690	ν C_4=O uridine (H-bonded)
	1678	1678	1678	ν C_4=O uridine (not H-bonded)
1650		1648	1645	δ NH_2 + ν ring adenosine
	1610	1610	1610	ν ring uridine
1602		1603	1602	ν ring + δ NH_2 adenosine
1576		1578	1577	ν ring adenosine

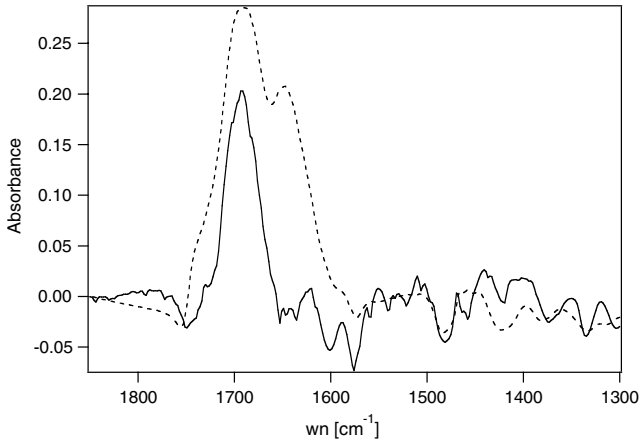

Figure 6. Difference of infrared absorption spectra of mixture POPA:POPU 1:1 (solid line) and mixture POPA:POPU 1:2 (dashed line) bilayers at lipid/water 80/20 % (w/w).

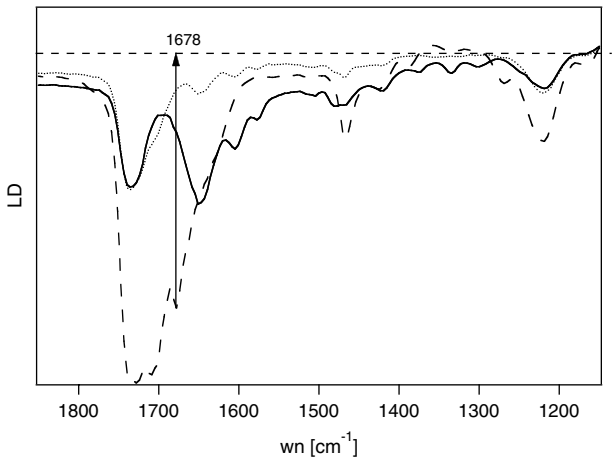

Figure 7. Linear dichroism spectra of POPA (solid line), POPU (dashed line) and, their 1:1 mixture (dotted line) for an incident angle 40° in the region 1900–1150 cm^{-1}.

To extract the desired information from these spectra two different methods were used: the first procedure was to deconvolve the bands by Gaussian functions. The number and corresponding wavenumber of the Gaussian contributions were chosen according to the current IR literature for nucleic acids and lipids. Table 3 shows the fitting results (fitting curves are not shown).

The second method was a weighted subtraction of the spectra of the pure nucleolipids from the spectra of the mixtures (figure 6); the weight was the relative quantity in the mixture. The difference spectra show mainly a positive band at 1690 cm^{-1}. This value is assigned to the C_4=O carboxylic stretching vibration of uridine when the bases are hydrogen bonded with adenosine or other complementary bases [39]. This is the direct evidence of the presence of selective H-bonding interactions in the mixture.

Another important feature concerns the POPA:POPU 1:2 sample, whose subtraction spectrum gives another absorption at 1650 cm^{-1}, in the region of adenosine NH_2 bending modes. This difference between the two mixtures can be probably understood considering the fact that, while in normal double-strand pairing one of the two H of NH_2 is involved in H-bonding with uridine, in mixtures polyU:polyA = 2:1 (i.e. the same composition we are observing) both H are involved in a simultaneous Watson–Crick and Hoogsten pairing to form a triple helix. This observation correlates well with the demixing that the DSC curves have highlighted for the 1:1 sample in the gel phase, where the formation of a POPU-rich complex seems likely.

Therefore, we can expect that if the bases are H-bonding in the membranes with the same specificity and stoichiometry as in nucleic acids this additional feature in the difference spectrum derives from a POPU–POPA–POPU complex.

On the basis of these results, we used vibrational infrared linear dichroism (VLD) to investigate the local arrangement of the mixed membranes. This technique provides information both on the orientation of a given transition dipole moment and on the mesoscopic ordering [16, 40–42].

Figure 7 shows VLD spectra collected for POPA, POPU and their mixed bilayers. The main difference between the dichroic spectra of binary and ternary phases is, first of all, the intensity of the dichroic signal, stronger for POPU bilayers with respect to POPA and mixtures. This is perfectly related to the different mosaicity obtained from neutron diffraction. POPU bilayers have a better long-range order than the other bilayers [17]. Moreover, we would like to highlight the band

centered at 1678 cm^{-1}, that is the C_4=O uridine stretching mode when H-bonded, which is lost in the mixture. Since the dichroic signal indicates the order and the orientation of a particular vibration mode with respect to the bilayer normal, it is possible to conclude that this C_4=O has no preferential orientation in the mixture with respect to binary POPU membranes as a consequence of H-bonding with adenosine.

4. Conclusion

This paper presents a neutron diffraction study of mixed POPU and POPA lamellar phases, for different molar ratios of the two nucleolipids. The binary systems (POPA and POPU) have different lyotropic behavior in terms of spontaneous water sorption and base orientation with respect to the membrane plane. The mixed systems display a structural modulation, that is a lower smectic period and a higher lipid cross-sectional area. This could indicate selective interactions between like-charged polar heads. DSC and FTIR techniques have provided convincing evidence that the slight structural variations emerging from neutron diffraction are actually related to base–base interactions that occur with the same stoichiometry as in nucleic acids.

Acknowledgments

Financial support from EU-FP6 (AMNA NMP4-CT-2004-013575), the European Union for the neutron diffraction measurements (RII3-CT-2003-505925), CSGI and MIUR (PRIN-2006) is acknowledged.

References

[1] Fuhrhop J H and Koning J 1994 *Membranes and Molecular Assemblies: The Synkinetic Approach* (London: Royal Society of Chemistry)
[2] Luk Y Y and Abbott N L 2002 Applications of functional surfactants *Curr. Opin. Colloid Interface Sci.* **7** 267–275
[3] Berti D and Baglioni P 2006 Self assembly of biologically inspired amphiphiles *Curr. Opin. Colloid Interface Sci.* **110** 74–8
[4] Bonini M *et al* 2005 Surfactant aggregates hosting a photoresponsive amphiphile: structure and photoinduced conformational changes *Soft Matter* **6** 444–54
[5] Ambrosi M *et al* 2006 Nanotubes from a vitamin C-based Bolaamphiphile *J. Am. Chem. Soc.* **128** 7209–14
[6] Tu R S and Tirrell M 2004 Bottom-up design of biomimetic assemblies *Adv. Drug Deliv. Rev.* **56** 1537–63
[7] Rosemeyer H 2005 Nucleolipids: natural occurrence, synthesis, molecular recognition, and supramolecular assemblies as potential precursors of life and bioorganic materials *Chem. Biodiversity* **2** 977–1063
[8] Baglioni P and Berti D 2003 Self assembly in micelles combining stacking and H-bonding *Curr. Opin. Colloid Interface Sci.* **8** 55–61
[9] Baldelli Bombelli F *et al* 2002 Giant polymerlike micelles formed by nucleoside-functionalized lipids *J. Phys. Chem.* B **106** 11613–21
[10] Banchelli M, Berti D and Baglioni P 2007 Molecular recognition drives oligonucleotide binding to nucleolipid self-assemblies *Angew. Chem.* **47** 3070–3
[11] Milani S *et al* 2007 Nucleolipoplexes: a new phospholipid bilayer-nucleic acid interaction *J. Am. Chem. Soc.* **129** 11664–5
[12] Berti D 1996 *Reactivity and Molecular Recognition in Organized System* (Florence: University of Florence)
[13] Shuto S, Ueda S, Fukukuawa K, Imnamura S, Matsuda A and Ueda T 1987 A facile one-step synthesis of 5′-phosphatidylnucleosides by an enzymatic two-phase reaction *Tetrahedron Lett.* **28** 199
[14] Shuto S *et al* 1988 A facile enzymatic synthesis of 5′-(3-sn-phosphatidyl)nucleosides and their antileukemic activities *Chem. Pharm. Bull.* **36** 209
[15] Franks N P and Lieb W R 1979 The structure of lipid bilayers and the effects of general anaesthetics: an x-ray and neutron diffraction study *J. Mol. Biol.* **133** 469–500
[16] Holmgren A, Johansson L B Å and Lindblom G 1987 An FTIR linear dichroism study of lipid membranes *J. Phys. Chem.* **91** 5298–301
[17] Milani S *et al* 2006 Structural investigation of bilayers formed by 1-Palmitoyl-2-oleoylphosphatidylnucleosides *Biophys. J.* **90** 1260–9
[18] Berti D *et al* 1998 Base complementarity and nucleoside recognition in phosphatidylnucleoside vesicles *J. Phys. Chem.* B **102** 303–8
[19] Cevc G 1993 *Phospholipids Handbook* (New York: Dekker)
[20] Solie T N and Schellman J A 1968 The interaction of nucleosides in aqueous solution *J. Mol. Biol.* **33** 61
[21] McElhaney R N 1982 The use of differential scanning calorimetry and differential thermal analysis in studies of model and biological membranes *Chem. Phys. Lipids* **30** 229–59
[22] Blume A 1991 Biological calorimetry: membranes *Thermochim. Acta* **193** 299–347
[23] Cheng W H 1980 A theoretical description of phase diagrams for nonideal lipid mixtures *Biochim. Biophys. Acta* **600** 358–66
[24] Lewis R N A H and McElhaney R N 1992 The mesomorphic phase behavior of lipid bilayers *The Structure of Biological Membranes* 1st edn, ed P L Yeagle (Boca Raton, FL: CRC press) pp 74–155
[25] Mabrey S and Sturtevant M J 1976 Investigation of phase transitions of lipids and lipid mixtures by high sensitivity differential scanning calorimetry *Proc. Natl Acad. Sci.* **73** 3862–6
[26] Findlay E J and Barton G 1978 Phase behavior of synthetic phosphatidylglycerols and binary mixtures with phosphatidylcholines in the presence and absence of calcium ions *Biochemistry* **17** 2400–5
[27] Garidel P, Johansson L B Å and Blume A 1997 Nonideal mixing and phase separation in phosphatidylcholine-phosphatidic acid mixtures as a function of acyl chain length and pH *Biophys. J.* **72** 2196–210
[28] Garidel P and Blume A 1998 Miscibility of phospholipids with identical headgroups and acyl chain lengths differing by two methylene units: effects of headgroup structure and headgroup charge *Biochim. Biophys. Acta* **1371** 83–95
[29] Nibu Y, Inoue T and Motoda I 1995 Effect of headgroup type on the miscibility of homologous phospholipids with different acyl chain lengths in hydrated bilayer *Biophys. Chem.* **56** 273–80
[30] Nibu Y and Inoue T 1995 Miscibility of binary phospholipid mixtures under hydrated and non-hydrated conditions. IV. Phosphatidylglycerols with different acyl chain length *Chem. Phys. Lipids* **76** 181–91
[31] Lindqvist M *et al* 2000 Optical spectroscopic study of effects of a single deoxyribose substitution in ribose backbone: implications in RNA–RNA interaction *Biochemistry* **39** 1693–701

[32] Kyogoku Y, Lord R C and Rich A 1967 An infrared study of hydrogen bonding between adenine and uracil derivatives in chloform solution *J. Am. Chem. Soc.* **89** 496–504
[33] Ivanov A Y *et al* 2003 Conformational structures and vibrational spectra of isolated pyrimidine nucleosides: Fourier transform infrared matrix isolation study of 2-deoxyuridine *Spectochim. Acta* A **59** 1959–73
[34] Liquier J and Taillanddier E 1996 Infrared spectroscopy of nucleic acid *Infrared Spectroscopy of Biomolecules* ed D Chapman (New York: Wiley–Liss) pp 131–58
[35] Saenger W 1984 *Principle of Nucleic Acid Structure* (New York: Springer)
[36] Banyay M, Sarkar M and Graslund A 2003 A library of IR bands of nucleic acids in solution *Biophys. Chem.* **104** 477–88
[37] Miles H T and Frazier J 1978 Infrared spectroscopy of polynucleotides in the carbonyl region in H_2O solution: AU systems *Biochemistry* **17** 2920–7
[38] Fringeli U P and Gunthard H H 1981 Infrared membrane spectroscopy *Membrane Spectroscopy* ed E Grell (Berlin: Springer)
[39] Miles H T 1964 The structure of three-stranded helix, poly (A+2U) *Proc. Natl Acad. Sci.* **51** 1104–9
[40] Binder H and Gawrisch K 2001 Effect of unsaturated lipid chains on dimensions, molecular order and hydration of membranes *J. Phys. Chem.* B **105** 12378–90
[41] Nillson A, Holmgren A and Lindblom G 1994 An FTIR study of the hydration and molecular ordering at phase transitions in the monooleoylglycerol/water system *Chem. Phys. Lipids* **71** 119
[42] Johansson L B Å and Lindblom G 1980 Orientation and mobility of molecules in membranes studied by polarized light spectroscopy *Q. Rev. Biophys.* **13** 63